

# Electromagnetic Detection of Buried Dielectric Targets

John Schneider, John Brew, *Member, IEEE*, and Irene C. Peden, *Life Fellow, IEEE*

**Abstract**—Scattering from subsurface objects is studied using the  $T$ -matrix method. The scatterer is represented as a dielectric ellipsoid and the source is assumed to be an electric dipole in a borehole. This approach easily accommodates rotations of the scatterer relative to the source and also permits relaxation of the two-dimensional constraint inherent in some models. In addition, it provides a new framework from which a large number of subsurface scattering problems can be studied.

To illustrate how this approach can be applied, the fields scattered from highly eccentric ellipsoids are found. These ellipsoids, which are presented as an approximation to cylindrical tunnels, are nonaxially symmetric. Results demonstrate the importance of using nonaxially symmetric scatterers rather than those that are axially symmetric. In addition, polarization results demonstrate that a method based on the polarization of the scattered field may provide a more robust diagnostic of scatterer location than methods using only a single field component.

An experiment based on a scale model of a subsurface tunnel is described. Results from the analytic model compare favorably with those obtained from the experiment. Results from the analytic model are also compared to those from a previously reported two-dimensional theory.

## I. INTRODUCTION

RECENTLY, there has been much interest in subsurface exploration at sites where boreholes are present [1], [2]. A cross-borehole technique has been used successfully at such sites to locate tunnels surrounded by hard rock (e.g., [3]). However, to date no satisfactory theoretical model exists that can fully accommodate the variety of situations found in the actual field environment. This paper presents a technique for studying subsurface scattering utilizing the  $T$ -matrix method; this technique is a more general approach than many previously reported. An arbitrary orientation of the source relative to the scatterer is allowed, an electric dipole is formulated as the source, and the scatterer is approximated as an ellipsoid.

Manuscript received July 27, 1990; revised March 8, 1991. This work was partially supported by the U.S. Army Belvoir Research, Development, and Engineering Center, Ft. Belvoir, VA, under Contract No. 62-4715, and by the National Science Foundation through Grant NSF 8408046.

J. Schneider is with the School of Electrical Engineering and Computer Science, Washington State University, Pullman, WA 99164.

J. Brew is with the Department of Electrical Engineering, FT-10, University of Washington, Seattle, WA 98195.

I. C. Peden is with the Department of Electrical Engineering, University of Washington, Seattle, WA 98195. She is presently on leave at the National Science Foundation, Division of Electrical and Communication Systems, Room 1151, 1800 G Street, NW, Washington, DC 20550.

IEEE Log Number 9100479.

The air-ground interface is assumed to be sufficiently distant from the scatterer so that it can be neglected.

Several authors have reported using the  $T$ -matrix to study the fields scattered from axially symmetric objects both in free space and in the earth [4]–[12]. The  $T$ -matrix method has much simpler solutions for axially symmetric objects than for nonaxially symmetric objects. However, it has been shown that for scatterers in free space, even slight asymmetries in the scattering object can have a large effect on the scattered field when the object is in the resonance region [13]. This fact motivated the choice of an ellipsoid, which in general does not have axial symmetry, to model the subsurface scatterer. As will be shown, removal of the axially symmetric constraint makes a significant difference for certain exploration problems.

Many antennas used for down-hole exploration have a radiation pattern similar to that of an electric dipole. Thus in the model an electric dipole is used as the source.

The next section provides an outline of the  $T$ -matrix method and discusses its use in the current formulation. Section III examines the field scattered from a highly eccentric ellipsoid. The parameters are chosen so the ellipsoid can approximate an air-filled tunnel in hard rock. The use of a nonaxially symmetric scatterer is shown to be significant. In Section IV, the scale model used to validate the theoretical model is discussed. Also, using parameters consistent with those for the scale model, results from the analytic model are compared to those of a previously reported two-dimensional model. Concluding remarks are given in Section V.

## II. THE $T$ -MATRIX METHOD

The  $T$ -matrix method was originally formulated by Waterman [14] to solve for the fields scattered from a perfectly conducting object of finite size. The method was later extended to dielectric scatterers [4], [5]. The  $T$ -matrix method was further extended by Kristensson and Ström [10], [11] to solve geophysical problems in which the air-ground interface or stratifications in the subsurface medium make significant contributions. In this study the air-ground interface and any stratifications are considered to be sufficiently distant from the scatterer so that the extensions provided by Kristensson and Ström are not necessary. The  $T$ -matrix method is primarily used in the resonance region, where approximate theories no longer pertain.

The  $T$ -matrix method is formulated using the dyadic Green's function together with the vector wave equation and the vector Green's theorem to obtain an integral equation that expresses the total electric field in terms of the incident field and the fields on the surface of the scattering object:

$$\begin{aligned} \vec{E}^i(\vec{r}') \cdot \vec{a} + \int_S dS \hat{n}(\vec{r}) \cdot ((\nabla \times \vec{E}) \times (\vec{G}_0 \cdot \vec{a}) \\ + \vec{E} \times \nabla \times (\vec{G}_0 \cdot \vec{a})) \\ = \begin{cases} \vec{E}(\vec{r}') \cdot \vec{a}, & \text{for } \vec{r}' \in V_0 \\ 0, & \text{for } \vec{r}' \in V_1 \end{cases} \end{aligned} \quad (1)$$

where  $\vec{E}$  is the total electric field,  $\vec{E}^i$  is the incident electric field,  $\vec{G}_0$  is the dyadic Green's function in the host medium,  $\vec{a}$  is an arbitrary vector,  $\vec{r}'$  is the observation point,  $\hat{n}$  is the outward unit normal vector,  $V_0$  is exterior to the scatterer, and  $V_1$  is interior. The integral is taken over the surface  $S$  of the object (see Fig. 1). If the observation point is in  $V_0$ , then the right-hand side of (1) is the total electric field. For an observation point in  $V_1$  the right-hand side is zero and thus the surface integral can be identified as the negative of the incident field. By making use of Maxwell's equations and dropping the arbitrary vector  $\vec{a}$ , one obtains an expression for the scattered field (the difference of the total field and incident field) and the incident field in terms of the surface integral. Thus, (1) yields:

$$\vec{E}^s = \int_S dS (i\omega\mu \hat{n} \times \vec{H} \cdot \vec{G}_0 + \hat{n} \times \vec{E} \cdot \nabla \times \vec{G}_0) \quad (2)$$

$$-\vec{E}^i = \int_S dS (i\omega\mu \hat{n} \times \vec{H} \cdot \vec{G}_0 + \hat{n} \times \vec{E} \cdot \nabla \times \vec{G}_0) \quad (3)$$

where  $\vec{E}^s$  is the scattered field. The incident field and the dyadic Green's function are known, while the surface fields and the scattered field are unknown. The remaining steps in the formulation of the  $T$ -matrix method can now be summarized as follows: (3) is used to solve for the unknown surface fields. Once known, the surface fields,  $\hat{n} \times \vec{H}$  and  $\hat{n} \times \vec{E}$ , are then used in (2) to solve for the scattered field. To accomplish this, (2) and (3) are rewritten with all the fields plus the dyadic Green's function expanded in a series of vector spherical harmonics [15], where the appropriate representation is dependent on the location of the observation point. Next, the order of integration and summation is interchanged, rendering two matrix equations from which the surface fields can be eliminated. A matrix, known as the transition or  $T$ -matrix, is then obtained which directly relates the incident field to the scattered field. The details involved in carrying out this operation can be found in [4]. The formulation for an ellipsoidal scatterer is presented in [13].

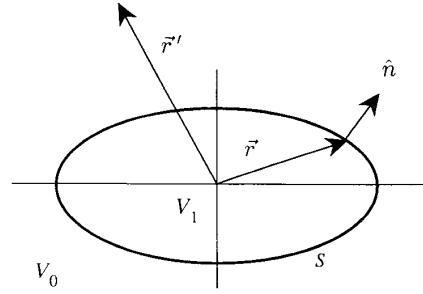


Fig. 1. Representation of the scatterer and the associated quantities used in the formulation of the  $T$ -matrix method. The surface of the scatterer is  $S$ ,  $V_1$  is interior to the scatterer,  $V_0$  is exterior,  $\vec{r}'$  is the observation point,  $\vec{r}$  is a point on  $S$ , and  $\hat{n}$  is the surface normal vector.

With the  $T$ -matrix method, angular variations of the source relative to the scatterer are available through the use of a relatively simple rotation operator. Therefore, the  $T$ -matrix can initially be calculated in the coordinate system natural to the scatterer and rotations realized through the use of this operator. The equations needed to calculate this rotation operator are given in Appendix A.

For the model developed in this study, dipole illumination is assumed. The needed basis function expansion for a dipole source is obtained by first assuming that the dipole source exists at the origin. This yields an incident field given by the  $\vec{N}_{01}$  vector spherical harmonic. The dipole is then translated to its actual location via the translation addition theorem for vector spherical harmonics [17]. The equations needed to express the incident field in an appropriate expansion are given in Appendix B. The incident field is then multiplied by the  $T$ -matrix to obtain the scattered field. The sum of the incident and scattered field yields the total field.

The cross section of an ellipsoid can only approximate the cross section of a tunnel that might be found in practice. However, unlike axially symmetric scatterers, an ellipsoid has a preferred scattering direction and is, therefore, believed to serve as a useful general model. The effects of features in the cross section of the tunnel, such as sharp corners and rough edges, are filtered by the surrounding medium.

An ellipsoid does not, in general, have axial symmetry and yet it possesses a symmetry that can be exploited in the calculation of the elements of the  $T$ -matrix [4]. This symmetry permits the creation of a computationally efficient code and was utilized in the development of the code needed for this study [13]. Nevertheless, a computational cost, which must be justified, is incurred by choosing an object lacking rotational symmetry. The results presented in the following section provide this justification.

### III. SCATTERING FROM ELLIPSOIDS

Lytle *et al.* [3] reported success in using a cross-borehole electromagnetic technique to pinpoint the location of tunnels in hard rock to within several centimeters of the surveyed location. The tunnels had cross-sectional dimen-

sions on the order of 2 m and were shaped approximately like the domed tunnel shown in Fig. 2. To determine the tunnel location, Lytle *et al.* employed continuous wave VHF signals (30 to 300 MHz), vertical electric dipole antennas, and a number of borehole loggings. The received signal, which was approximately the vertical component of the electric field, provided the diagnostic for the tunnel location. Several "ideal" features existed in the test cases of [3] that cannot be assumed to exist in the general field environment; e.g., vertical alignment of the boreholes and a tunnel axis perpendicular to the plane of the boreholes. However, the initial success of this cross-borehole probing provides motivation for the development of a more general theoretical framework from which to investigate this problem.

In this section the field scattered from a highly eccentric ellipsoid is found. The constitutive parameters and dimensions are chosen so that this ellipsoid can be used to approximate the infinitely long, cylindrical, air-filled tunnel surrounded by hard rock used in [3]. The frequency of illumination is assumed to be in the VHF range, throughout which the host medium is assumed to have a relative permittivity  $\epsilon_r$  of 9, a conductivity  $\sigma$  of 0.002 S/m, and a relative permeability  $\mu_r$  of 1. It is assumed that boreholes are present in the vicinity of a scatterer so deeply buried that the air-ground interface can be neglected. Fig. 3 shows a cross-sectional view of the assumed geometry. Finally, it is assumed that the transmitter and receiver are moved along the boreholes at the same depth and rate. In practice, for a given logging, constant offsets in the depths of the two antennas can be maintained.

Fig. 2 gives diagrammatical views of a segment of a realistic tunnel shape and an ellipsoid used to model it. Although the ellipsoid is of finite extent, making it sufficiently eccentric provides a good approximation to the true tunnel cross section over a fairly large region. Attenuation in the host medium further justifies the use of an ellipsoid. By accurately approximating the tunnel in the vicinity of the transmitter borehole, a close approximation to the true scattered field can be obtained.

The field scattered from an air-filled ellipsoid 6.6-m long, 2.2-m high, and 1.82-m wide serves to demonstrate the need for a nonaxially symmetric scatterer. The diagrammatical view of this ellipsoid is drawn to scale in Fig. 2(b). Its volume is equal to that of a spheroid with the same length and a diameter of 2 m. The ellipsoid dimensions reflect a 10% increase in the "height" and a 10% decrease in the "width" of the spheroid, so its cross section is nearly circular, although its length-to-width ratio is over 3.6 to 1.

The solid curve of Fig. 4 shows the vertical component of the scattered field as a function of the elevation of the transmitter and receiver relative to the center of the ellipsoid. The frequency used, 60 MHz, corresponds to that of a previous study [3]; it also represents a significant component of the signal used in some time-domain detection schemes [18]. The results for four different rotation

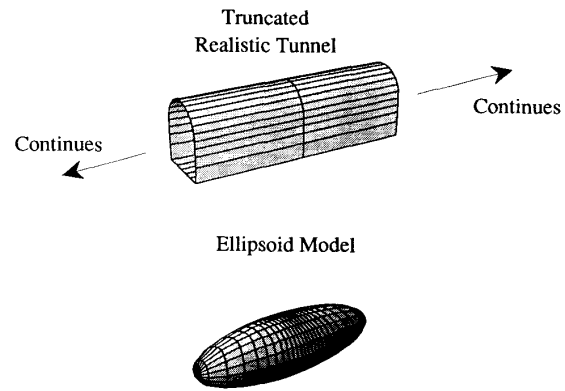


Fig. 2. Diagrammatical representation of a realistic tunnel and a corresponding ellipsoidal model.

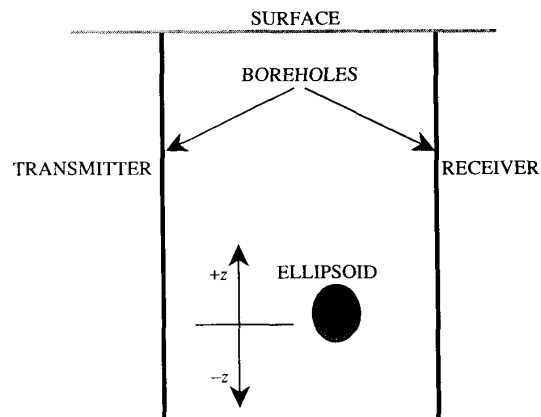


Fig. 3. Cross-sectional representation of the scatterer and borehole geometry.

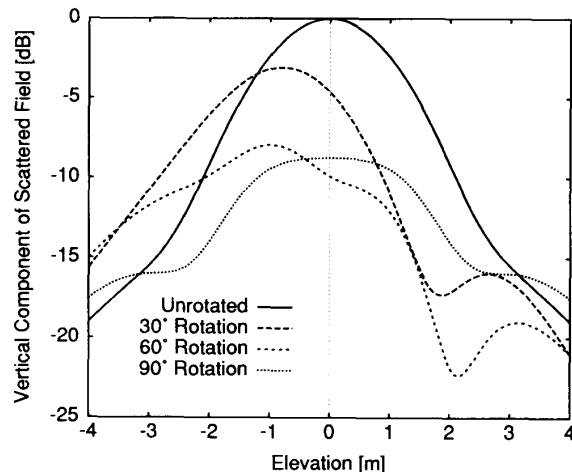


Fig. 4. Vertical component of the scattered field versus elevation relative to the center of the scatterer. Results are for an ellipsoidal scatterer with axial rotations of 0°, 30°, 60°, and 90°. The frequency used is 60 MHz.

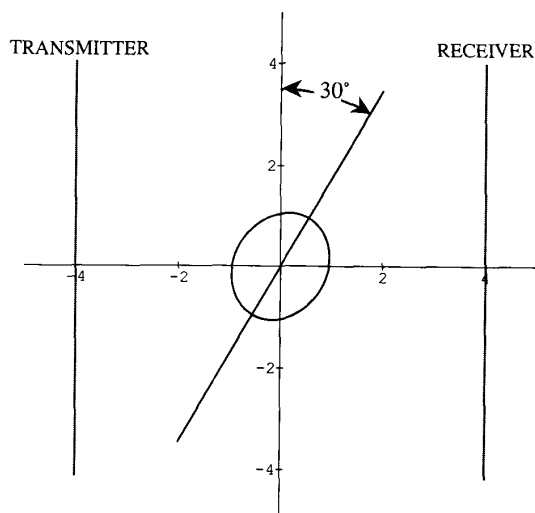


Fig. 5. Cross-sectional view of transmitter and receiver boreholes, and the ellipsoid with 30° axial rotation. All dimensions are in meters.

angles of the scatterer about the longitudinal axis (roll) are shown in Fig. 4, while Fig. 5 provides a cross-sectional view of the ellipsoid for an axial rotation of 30° and indicates the dimensions assumed. The rotation carries the top of the ellipsoid away from the transmitter.

Apart from differences in magnitude, the result obtained from the unrotated ellipsoid is nearly identical to that obtained by replacing the ellipsoid with a spheroid of the same volume. However, the scattered field of a spheroid remains the same under axial rotations. It is clear from Fig. 4 that this difference is significant. Therefore, modeling a scatterer lacking axial symmetry by an axially symmetric object can lead to erroneous results.

The results shown in Fig. 4 might be explained in part by the induction in the scatterer of a dipole perpendicular to its longitudinal axis. This induced dipole would tend to align with the preferred scattering direction of the ellipsoid and would account for the downward shift of the peak in the scattered field seen for the 30° and 60° rotations. The 0° and 90° rotations are similar, in that both produce scattered fields that are symmetric about the location of the center of the ellipsoid.

In practice, boreholes can have as much as 30° of drift from vertical. When the air-ground interface is ignored, this drift can be viewed as a rotation of the scatterer relative to the source. Thus it is important to consider the 30° axial rotation results. They have a significant effect on the scattered field over a large range of borehole separations, even though this effect tends to diminish with increased separation or lower frequencies.

Rotations of the longitudinal axis of the scatterer about the other two axes of freedom—either horizontally away from the perpendicular to the plane containing the boreholes (yaw) or vertically (pitch)—also have an effect on the scattered field and can represent other possibilities for borehole drift. Physically, a dipole induced within the

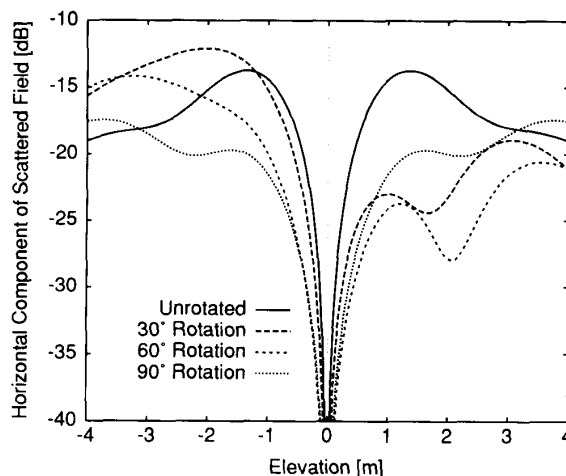


Fig. 6. Horizontal component of the scattered field versus elevation relative to the center of the scatterer. Results are for an ellipsoidal scatterer with axial rotations of 0°, 30°, 60°, and 90°.

scatterer accounts for some of the changes observed in the field scattered from objects with rotations of yaw or pitch. Although the effects of these two rotations are not as marked as those associated with roll, they cannot be ignored. In practice, any of these rotations can be present to some degree and the sum of their effects can have a large impact on the received field. The capability of this three-dimensional model to account for them is one of its important features.

With the *T*-matrix method the polarization of the scattered field can easily be determined. Fig. 6 shows the calculated magnitude of the horizontal component of the scattered field in the receiver borehole. Figs. 4 and 6 are plotted so that 0 dB corresponds to the maximum measured vertical component for the unrotated ellipsoid. The horizontal and vertical components of the scattered fields for the ellipsoids are asymmetric for 30° and 60° rotations. However, the rotations do not affect the position of the null in the horizontal field. Therefore, the horizontal component, together with the vertical component of the scattered field, can be used for a more robust detection scheme than those which examine only the vertical component.

#### IV. SCALE MODEL

To provide validation for the analytical model, a laboratory scale model was constructed as described below. The experimental setup is shown in Fig. 7. A circular aluminum tank 135-cm in diameter and 90-cm in height was lined with microwave absorber and filled with a mixture of 93% alumina powder and 7% potting soil. A hollow cylindrical tube of cardboard with an outer diameter of 8.5-cm defined the void representing the tunnel. The boreholes, symmetrically placed 17 cm on either side of the tunnel, were defined by PVC tubes. Sleeve dipole antennas were used for both the transmitter and receiver;

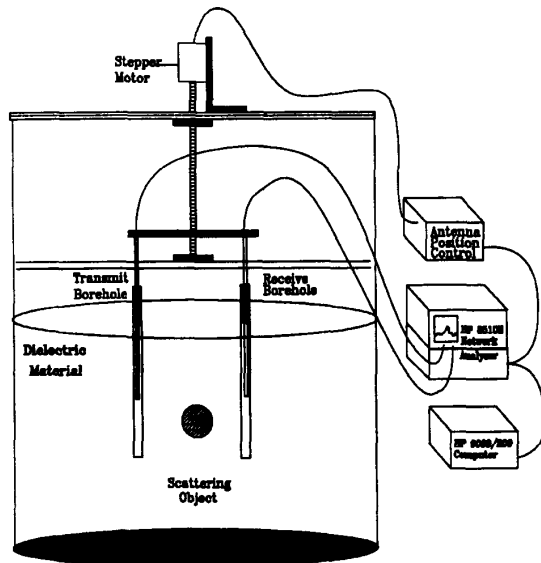
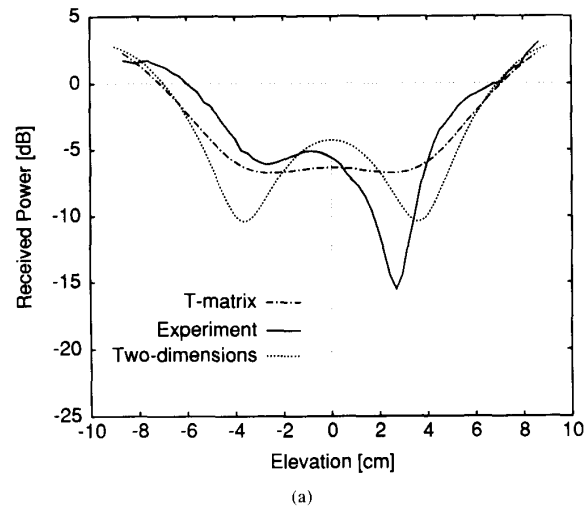


Fig. 7. Cross-borehole scattering experiment setup.

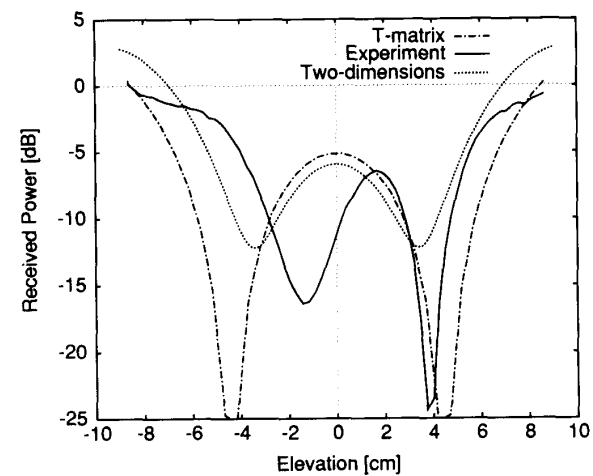
their measured radiation patterns were close to that of an infinitesimal electric dipole antenna. Cross-borehole field patterns were measured on an HP 8510B network analyzer. A personal computer was used to control both the positioning of the probes by means of a stepping motor and data acquisition through the network analyzer; it was also used for the archiving and manipulation of data. All measurements were made in the frequency domain and were done over the frequency range 2 to 4 GHz.

The constitutive parameters of the scale model were  $\epsilon_r = 3.2$ ,  $\sigma = 0.017$  S/m, and  $\mu_r = 1$ . These parameters were used in the analytical model and assumed to be constant over the 2 to 4 GHz range.

Fig. 8(a) and (b) shows a comparison of the analytic and scale model results for the received power at two different frequencies. The received power was measured at a depth corresponding to that of the transmitter, covering a range from approximately  $-8$  to  $+8$  cm. Since the cardboard tube defining the tunnel shape had a circular cross section, a spheroid was used in the analytical model. This spheroid had a length of 26.5-cm and a diameter of 8.5 cm. In these figures the dash-dot line represents the calculated result, and the experimental result is shown as a solid line. At both frequencies the two curves have approximately the same shape. Time domain measurements indicated that the walls of the tank were not completely masked by the microwave absorbing material. Additionally, a series of range calibration measurements showed that a standing wave was present in the tank when CW illumination was used. However, practical considerations in the construction of the experiment restricted the size of the tank and scatterer, the frequency of illumination, and the constitutive parameters of the medium. These restrictions limited the degree to which effects of the tank walls



(a)



(b)

Fig. 8. Comparison of results from the analytic and scale models at two different frequencies. Plots show the vertical component of the received field versus elevation. (a) 2.64 GHz. (b) 2.69 GHz.

could be reduced. These effects account for most of the discrepancies between theoretical and experimental results.

Fig. 8(a) and (b) also shows the results for a two-dimensional approach [19]. These results change relatively little with frequency. The *T*-matrix method is seen to predict the received power about as well as the two-dimensional approach. Results from the two-dimensional theory and the *T*-matrix method have been compared over a larger range of elevations than shown in Fig. 8 and over many different frequencies. These comparisons demonstrate that both the two-dimensional and *T*-matrix three-dimensional models provide similar diagnostic information, with the latter additionally able to accommodate situations in which the angular relationship between borehole and tunnel orientation varies.

### V. CONCLUSIONS

In this study the  $T$ -matrix method was used to determine the field scattered from an ellipsoid illuminated by an electric dipole in a lossy host medium. The  $T$ -matrix method is a three-dimensional technique and, unlike two-dimensional approaches, can predict changes in the field due to arbitrary rotations of the scatterer. In addition, the dipole source provides an accurate representation of the transmitting antenna often used in down-hole exploration. These two features enable the study of the field scattered from a subsurface target in the presence of boreholes.

The results presented indicate the importance of the use of a nonaxially symmetric scatterer to represent asymmetric targets. The field scattered from an axially symmetric scatterer such as a spheroid does not change with axial rotation of the scatterer; for parallel boreholes, it is always symmetric relative to the center of the scatterer. However, the vertical component of the electric field scattered from a nonaxially symmetric scatterer such as an ellipsoid becomes asymmetric as the scatterer is rotated, and the maximum field strength shifts away from the center of the scatterer. In addition, polarization studies show that the horizontal component of the scattered field is insensitive to either borehole drift or axial rotations of the scatterer.

The  $T$ -matrix results were compared to those from a laboratory scale-model experiment of a subsurface tunnel. They were also compared with those from a more conventional two-dimensional approach. The  $T$ -matrix results compared favorably with those of the scale model while providing all the diagnostic capabilities of the two-dimensional approach.

### APPENDIX A

To determine the rotation operator, vector spherical harmonics in the coordinate system natural to the scatterer must be related to those in the principal frame of reference. Let an Eulerian rotation of  $\alpha$ ,  $\beta$ ,  $\gamma$  transform the primed coordinate system, which is natural to the scatterer, into the unprimed coordinate system, which corresponds to the principal frame of reference. Then, using the notation of Tsang *et al.* [16] and the work of Edmonds [17], a relationship between the spherical harmonics  $Y_n^m$  can be expressed in terms of the rotation group representation  $\mathcal{D}_{\mu m}^{(n)}(\alpha\beta\gamma)$ . This relationship is given by:

$$\zeta_{mn} Y_n^m(\theta', \phi') = \sum_{\mu=-n}^n \zeta_{\mu n} Y_n^{\mu}(\theta, \phi) \mathcal{D}_{\mu m}^{(n)}(\alpha\beta\gamma) \quad (4)$$

where

$$\mathcal{D}_{\mu m}^{(n)}(\alpha\beta\gamma) = e^{i\mu\gamma} d_{\mu m}^{(n)}(\beta) e^{im\alpha} \quad (5)$$

$$d_{\mu m}^{(n)} = \sum_{\sigma} \frac{[(n+m)!(n-m)!(n+\mu)!(n-\mu)!]}{\sigma!(m+\mu+\sigma)!(n-m-\sigma)!(n-\mu-\sigma)!} \cdot (-1)^{n-\mu-\sigma} \left(\sin \frac{\beta}{2}\right)^{2n-2\sigma-\mu-m} \left(\cos \frac{\beta}{2}\right)^{2\sigma+\mu+m} \quad (6)$$

and

$$\zeta_{mn} = \left( \frac{(2n+1)(n-m)!}{4\pi n(n+1)(n+m)!} \right)^{1/2}. \quad (7)$$

The limits of the  $\sigma$  summation in (6) are such that all the factorials are non-negative. Using (4) and the orthogonality relation,

$$\sum_{\xi=-n}^n \mathcal{D}_{\mu\xi}^{-1(n)}(\alpha\beta\gamma) \mathcal{D}_{\xi m}^{(n)}(\alpha\beta\gamma) = \delta_{\mu m} \quad (8)$$

where  $\delta_{\mu m}$  is the Kronecker delta, the  $\vec{N}_{mn}$  vector spherical harmonics in the two coordinate systems are related by:

$$\vec{N}_{mn}(kr, \theta', \phi') = \sum_{\mu=-n}^n \vec{N}_{\mu n}(kr, \theta, \phi) \mathcal{D}_{\mu m}^{(n)}(kr, \theta, \phi) \quad (9)$$

$$\vec{N}_{\mu n}(kr, \theta, \phi) = \sum_{m=-n}^n \vec{N}_{\mu n}(kr, \theta', \phi') \cdot \mathcal{D}_{m\mu}^{-1(n)}(kr, \theta, \phi) \quad (10)$$

where

$$\mathcal{D}_{\mu m}^{-1(n)}(\alpha\beta\gamma) = e^{-i\mu\gamma} d_{\mu m}^{(n)}(-\beta) e^{-im\alpha}. \quad (11)$$

Similar expressions relate the  $\vec{M}_{mn}$  harmonics. Using a double bar to indicate a matrix, the  $T$ -matrix calculated in the primed coordinate system  $\vec{T}'$  can be related to the  $T$ -matrix in the principal frame  $\vec{T}$  by:

$$\vec{T} = \vec{D} \vec{T}' \vec{D}^{-1} \quad (12)$$

where

$$\vec{D} = \begin{bmatrix} \vec{\mathcal{D}} & 0 \\ 0 & \vec{\mathcal{D}} \end{bmatrix}. \quad (13)$$

The elements of  $\mathcal{D}$  are given by:

$$(\vec{\mathcal{D}})_{mn\mu\nu} = \delta_{n\nu} \mathcal{D}_{\mu m}^{(n)}(\alpha\beta\gamma) \quad (14)$$

where  $m$  and  $n$ , the subscripts associated with one set of vector spherical harmonics, are mapped into the row number by  $r = n(n+1) + m$ , and  $\mu$  and  $\nu$ , the other set of subscripts, are mapped into a column number by  $c = \nu(\nu+1) + \mu$ . The matrix  $\vec{D}^{-1}$  is the inverse of  $\vec{D}$  and is given by:

$$\vec{D}^{-1} = \begin{bmatrix} \vec{\mathcal{D}}^{-1} & 0 \\ 0 & \vec{\mathcal{D}}^{-1} \end{bmatrix}. \quad (15)$$

where the elements of  $\vec{\mathcal{D}}^{-1}$  are given by

$$(\vec{\mathcal{D}}^{-1})_{mn\mu\nu} = \delta_{n\nu} \mathcal{D}_{\mu m}^{-1(n)}(\alpha\omega\gamma). \quad (16)$$

For a given scattering object, the  $\vec{T}'$  need only be calculated once. For every rotation, both  $\vec{D}$  and  $\vec{D}^{-1}$  have to be recalculated. However, the elements of these matrices are seen to consist of a simple product of trigonometric functions and complex exponents and can be calculated quite readily.

## APPENDIX B

In order to derive the vector spherical harmonic expansion for an electric dipole which is not at the origin, consider the translation addition theorem for  $\vec{N}_{01}$ , which is a special case of the general translation addition theorem for  $\vec{N}_{mm}$ . The translation addition theorem gives a relationship between the vector spherical harmonics in one coordinate system to those of another coordinate system [17]. Let the three vectors  $\vec{r}$ ,  $\vec{r}'$ , and  $\vec{r}_0$  form a triangle such that:

$$\vec{r} = \vec{r}' + \vec{r}_0. \quad (17)$$

As shown in Fig. 9, the vectors  $\vec{r}$  and  $\vec{r}_0$  have an origin of  $O$ , while the vector  $\vec{r}'$  has an origin of  $O'$ . The vector  $\vec{r}_0$  points from the origin  $O$  to the  $O'$  origin. Let the dipole be located at the origin  $O$  and the  $T$ -matrix for the scatterer be evaluated using its natural origin  $O'$ . The vector spherical harmonic  $\vec{N}_{01}(k\vec{r})$ , which assumes an origin  $O$ , is the appropriate expression for the fields radiated from a dipole. The goal is to express  $\vec{N}_{01}(k\vec{r})$  in terms of vector spherical harmonics that are functions only of  $\vec{r}'$  and the constant  $\vec{r}_0$ . This gives the incident field expressed in terms of the coordinate system natural to the scatterer. The needed relation follows directly from the translation addition theorem and is given by [16]:

$$\begin{aligned} \vec{N}_{01}(k\vec{r}) = & \sum_{\nu=1}^{\infty} \sum_{\mu=-\nu}^{\nu} \{B_{\mu\nu 01}(k\vec{r}_0) Rg\vec{M}_{\mu\nu}(k\vec{r}') \\ & + A_{\mu\nu 01}(k\vec{r}_0) Rg\vec{N}_{\mu\nu}(k\vec{r}')\} \end{aligned} \quad (18)$$

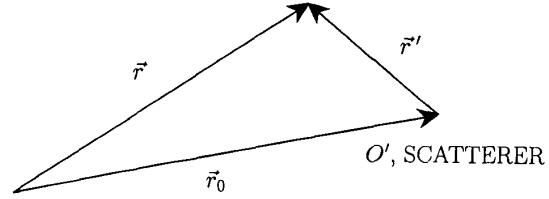
where

$$\begin{aligned} A_{\mu\nu 01}(k\vec{r}_0) = & \frac{\zeta_{01}}{\zeta_{\mu\nu}} (-1)^{\mu} \sum_p a(0, 1 | -\mu, \nu | p) \\ & \cdot a(1, \nu, p) h_p(kr_0) Y_p^{-\mu}(\theta_0, \phi_0) \end{aligned} \quad (19)$$

$$\begin{aligned} B_{\mu\nu 01}(k\vec{r}_0) = & \frac{\zeta_{01}}{\zeta_{\mu\nu}} (-1)^{\mu+1} \sum_p a(0, 1 | -\mu, \nu | p, p-1) \\ & \cdot b(1, \nu, p) h_p(kr_0) Y_p^{-\mu}(\theta_0, \phi_0) \end{aligned} \quad (20)$$

$$\begin{aligned} a(0, 1 | -\mu, \nu | p) & \\ = (-1)^{-\mu} (2p+1) & \left[ \frac{(\nu-\mu)! (p+\mu)!}{(\nu+\mu)! (p-\mu)!} \right]^{1/2} \\ \cdot \begin{pmatrix} 1 & \nu & p \\ 0 & -\mu & \mu \end{pmatrix} & \begin{pmatrix} 1 & \nu & p \\ 0 & 0 & 0 \end{pmatrix} \end{aligned} \quad (21)$$

$$\begin{aligned} a(0, 1 | -\mu, \nu | p, p-1) & \\ = (-1)^{-\mu} (2p+1) & \left[ \frac{(\nu-\mu)! (p+\mu)!}{(\nu+\mu)! (p-\mu)!} \right]^{1/2} \\ \cdot \begin{pmatrix} 1 & \nu & p \\ 0 & -\mu & \mu \end{pmatrix} & \begin{pmatrix} 1 & \nu & p-1 \\ 0 & 0 & 0 \end{pmatrix} \end{aligned} \quad (22)$$



$O$ , DIPOLE

Fig. 9. Relation of the vectors used in the translation addition theorem for vector spherical harmonics.

$$\begin{aligned} a(1, \nu, p) = & i^{\nu+p-1} \frac{1}{2\nu(\nu+1)} (1+2\nu) \\ & \cdot (2-p-p^2+\nu+\nu^2) \end{aligned} \quad (23)$$

$$\begin{aligned} b(1, \nu, p) = & -i^{\nu+p-1} \frac{2\nu+1}{2\nu(\nu+1)} [(2+\nu+p) \\ & \cdot (\nu+p-1)(1-\nu+p) \\ & \cdot (2+\nu+p)]^{1/2} \end{aligned} \quad (24)$$

where  $h_p$  is the spherical Hankel function of the first kind. In these equations the terms of the form:

$$\begin{pmatrix} 1 & j_2 & j_3 \\ 0 & m_2 & -m_2 \end{pmatrix} \quad (25)$$

represent a subset of the Wigner  $3j$  symbols. This subset is relatively simple to calculate and the governing formulas for the terms are given by [17]. In (19) and (20) there is a summation over  $p$ . This summation is carried out over all  $p$  that yield nonzero terms. Fortunately, the Wigner  $3j$  symbol as given by (25) is only nonzero for  $j_2 - 1 \leq j_3 \leq 1 + j_2$ , where the assumption has been made that  $j_2 \geq 1$ . This fact limits the values of  $p$  that must be considered in the summations for  $A_{\mu\nu 01}$  and  $B_{\mu\nu 01}$ . It can also be shown that  $A_{\mu\nu 01}$  is zero even when  $p = \nu$ . Therefore, for every value of  $\mu$  and  $\nu$  it is only necessary to sum  $A_{\mu\nu 01}$  and  $B_{\mu\nu 01}$  over two values of  $p$ ; namely,

$$A_{\mu\nu 01} \neq 0, \quad \text{for } p = \begin{cases} \nu+1 \\ \nu-1 \end{cases} \quad (26)$$

$$B_{\mu\nu 01} \neq 0, \quad \text{for } p = \begin{cases} \nu+1 \\ \nu \end{cases} \quad (27)$$

Using these expressions for a dipole specified at a location away from the scatterer, the vector spherical harmonic expansion of the incident field in the  $O'$  coordinate system, which is natural to the scatterer, can be obtained. Equation (18) is used to generate the desired number of terms. For example, if a  $T$ -matrix with a dimension of  $240 \times 240$  were used in the formulation of a problem, the specified value of  $\vec{r}_0$  would be used in (18) and  $\nu$  would

vary from one to ten, with  $\mu$  varying from  $-\nu$  to  $+\nu$ . The right-hand side of (18) gives all the needed vector spherical harmonics and their coefficients in the proper coordinate system; that is, natural to the scatterer.

#### REFERENCES

- [1] P. Maass, "S. Korean, U.S. officials find tunnel from north," *Washington Post*, Mar. 4, 1990.
- [2] "Belvoir equipment finds DMZ tunnel," *Pentagram*, Mar. 15, 1990.
- [3] R. J. Lytle, E. F. Laine, D. L. Lager, and D. T. Davis, "Cross-borehole electromagnetic probing to locate high-contrast anomalies," *Geophysics*, vol. 44, no. 10, pp. 1667-1676, 1979.
- [4] P. C. Waterman, "Symmetry, unitarity, and geometry in electromagnetic scattering," *Phys. Rev. D.*, vol. 3, no. 4, pp. 825-839, 1971.
- [5] P. Barber and C. Yeh, "Scattering of electromagnetic waves by arbitrary shaped dielectric bodies," *Appl. Opt.*, vol. 14, no. 12, pp. 2864-2872, 1975.
- [6] C. Yeh, S. Colak, and P. Barber, "Scattering of sharply focused beams by arbitrary shaped dielectric particles: An exact approach," *Appl. Opt.*, vol. 21, no. 24, pp. 4426-4433, 1982.
- [7] A. R. Holt, "Electromagnetic wave scattering by spheroids: A comparison of experimental and theoretical results," *IEEE Trans. Antennas Propagat.*, vol. AP-30, no. 4, pp. 758-760, 1982.
- [8] A. R. Holt, "The scattering of single hydrometeors," *Radio Sci.*, vol. 17, no. 5, pp. 929-945, 1982.
- [9] A. Mugnai and W. Wiscombe, "Scattering from nonspherical Tschebyshev particles. I: Cross sections, single scattering albedo, asymmetry factor and backscattered fraction," *Appl. Opt.*, vol. 25, no. 7, pp. 1235-1244, 1986.
- [10] G. Kristensson and S. Ström, "The  $T$ -matrix approach to scattering from buried inhomogeneities," in *Acoustic, Electromagnetic, and Elastic Wave Scattering—Focus on the  $T$ -Matrix Approach*. New York: Pergamon, 1979, pp. 135-167.
- [11] G. Kristensson and S. Ström, "Electromagnetic scattering from geophysical targets by means of the  $T$ -matrix approach: A review of some recent results," *Radio Sci.*, vol. 17, no. 5, pp. 903-912, 1982.
- [12] A. Karlsson and G. Kristensson, "Electromagnetic scattering from subterranean obstacles in a stratified ground," *Radio Sci.*, vol. 18, no. 3, pp. 345-356, 1983.
- [13] J. B. Schneider and I. C. Peden, "Differential cross section of a dielectric ellipsoid by the  $T$ -matrix, extended boundary condition method," *IEEE Trans. Antennas Propagat.*, vol. AP-36, no. 9, pp. 1317-1321, 1988.
- [14] P. C. Waterman, "Matrix formulation of electromagnetic scattering," *Proc. IEEE*, vol. 53, pp. 805-812, 1965.
- [15] J. A. Stratton, *Electromagnetic Theory*. New York: McGraw-Hill, 1941.
- [16] L. Tsang, J. A. Kong, and R. T. Shin, *Theory of Microwave Remote Sensing*. New York: Wiley, 1985.
- [17] A. R. Edmonds, *Angular Momentum in Quantum Mechanics*. Princeton, NJ: Princeton Univ. Press, 1957.
- [18] R. Greenfield, "Modeling of electromagnetic propagation between boreholes," in *Proc. 3rd Tech. Symp. Tunnel Detection* (Golden, CO), Jan. 1988.
- [19] J. H. Richmond, "TE-wave scattering by a dielectric cylinder of arbitrary cross-section shape," *IEEE Trans. Antennas Propagat.*, vol. AP-14, no. 4, pp. 460-464, 1966.



**John Schneider** received the B.S. degree in electrical engineering from Tulane University in 1983, and the M.S. and Ph.D. degrees in electrical engineering from the University of Washington in 1985 and 1991, respectively.

He is presently a faculty member in the School of Electrical Engineering and Computer Science at Washington State University, Pullman. His current research interests are in the areas of subsurface scattering of electromagnetic waves and the analysis of higher order spectra of nonlinear

systems.

Dr. Schneider is a member of Tau Beta Pi and Eta Kappa Nu.



**John Brew** (M'82) was born in Brooklyn, NY, on November 28, 1957. He received the B.S. degree in electrical engineering from the University of Washington, 1982, where he is currently pursuing the M.S. degree in electrical engineering.

From 1982 to 1985 he was an Electrical Engineer with the U.S. Navy. Since 1985 he has been employed by the Boeing Aerospace and Electronics Company as an Electrical Engineer. His current interests are remote sensing, electromagnetic compatibility, and wideband receiving systems.

Mr. Brew is a member of Tau Beta Pi.



**Irene C. Peden** (M'53-SM'62-F'74-LF'90) received the B.S. degree from the University of Colorado, Boulder, and the M.S. and Ph.D. degrees from Stanford University, Palo Alto, CA, all in electrical engineering.

She is Professor of Electrical Engineering at the University of Washington, Seattle, where she teaches courses in electromagnetic theory, wave propagation and transmission lines, and antennas, and carries out research in electromagnetic techniques in subsurface scattering and exploration, including tunnel detection.

Dr. Peden was the recipient of the 1988 IEEE Haraden Pratt Award, a 1984 Centennial Medal, and the 1989 Meritorious Achievement Award in Accreditation Activities of the Educational Activities Board. She was 1976 and 1977 Vice President for Educational Activities, and 1989 President of the Antennas and Propagation Society. She currently serves on the Awards Board as Chair of the Heinrich Hertz Medal Committee and on the Spectrum/Institute Advisory Board. She is a member of the Commission on Engineering and Technical Systems of the National Research Council, the Engineering Development Council of the University of Colorado, Boulder, and the Board of Visitors of the College of Engineering University of California, Davis. She is a member of the Defense Science Board and a former chair of the Army Science Board. She received the 1987 U.S. Army Distinguished Civilian Service Award, a 1974 Distinguished Engineering Alumnus Award-Education from the University of Colorado, and the 1973 Award of Achievement of the Society of Women Engineers. She is a Director of the Morrison Knudsen Corporation, and a Fellow of the American Association for the Advancement of Science, the Accreditation Board for Engineering and Technology, the Explorers' Club, and the Society of Women Engineers. Dr. Peden is presently on leave from the University of Washington to serve as Director of the Division of Electrical and Communications Systems to the National Science Foundation.